Identification of the IncRNA HIF1A-AS3 Biomarker and Analysis of Immune Infiltrates in Breast Cancer

Liyun Yong[1#]; Xiaoyan Lin[2#]; Xiaoxing Yin[1#]; Lu Cai[1]; Manuel A Luis[1]; Marcia R Dique[1]; Shasha Tang[1]*; Feng Feng Cai[1]*

[1]*Department of Breast Surgery, Tongji Hospital, School of Medicine, Tongji University, Shanghai, 200065, China.*

[2]*Department of Breast Surgery, Yangpu Hospital, School of Medicine, Tongji University, Shanghai, 200090, China.*

[#]*These authors have contributed equally to this work .*

Abstract

Breast Cancer (BC) is the predominant malignant tumor among women globally. It has high recurrence which have adverse effects on patient outcomes. Therefore, there is need to identify effective biomarkers for prognostic evaluation. Numerous long non-coding RNAs (lncRNAs) have been shown to be implicated in the regulation of BC tumorigenesis. The role of lncRNA Hypoxia-Inducible Factor 1 Alpha-antisense RNA 3 (HIF1A-AS3) in BC has not been studied. The purpose of this study was to find a novel biomarker that can guide the formulation of effective treatments. The Breast Cancer on The Cancer Genome Atlas (TCGA-BRCA) database was used to investigate the relationship between HIF1A-AS3 and BC, and R-packet analysis of RNA sequencing data was used to identify Differentially Expressed Genes (DEGs) between high and low HIF1A-AS3 expression BC tissues. The expression level of HIF1A-AS3 in various BC cells and normal breast cell, BC and paracancerous tissues from clinical patient samples, as well as primary breast cancer cell, respectively was analyzed. Kaplan-Meier (KM) and Cox regression analyses were used in this study to find the predictive value of HIF1A-AS3 on clinical outcomes in BC patients. The association between infiltration of HIF1A-AS3 and immune cells was determined through Spearman's correlation analyses. The results revealed that the expression of HIF1A-AS3 was significantly elevated in breast cancer cell, BC tissues and primary breast cancer cell compared with that in normal breast cell, paracancerous tissues, and primary breast epithelial cell. KM analysis showed that high expression of HIF1A-AS3 was associated with poor OS [Hazard Ratio (HR): 1.42, P=0.029], Progression-Free Interval (PFS) (HR:1.60, P=0.005), and DSS (HR:1.60, P=0.031). Moreover, analysis of immune infiltration showed that HIF1A-AS3 expression was associated with some types of immune infiltrating cells. In conclusion, elevated HIF1A-AS3 expression in breast cancer is correlated with adverse clinical outcomes and specific immune infiltrating cells, highlighting its potential as a prognostic biomarker and therapeutic target.

Keywords: HIF1A-AS3; Biomarker; Breast Cancer (BC); Immune Infiltration; Prognosis.

Introduction

Breast Cancer (BC) is a complex heterogeneous disease. Globally, it is the second leading cause of cancer-related deaths in women [1]. According to cancer statistics from the American Cancer Society, approximately 287,850 new cases of BC and 43,250 deaths due to BC occur in US women were reported in 2022 [2]. Recent advances in development of therapeutic drugs for cancer including chemotherapy, endocrine, and target therapy have led to a significant reduction in development of tumors and improved survival rates of patients with BC in the past three decades. However, drug resistance continues to be a major challenge to the prognosis of patients [3,4].

Currently, Estrogen Receptor (ER), Progesterone Receptor (PR), and Human Epidermal Growth Factor Receptor 2 (HER2) have been clinically used as the biomarkers for classification and prognosis evaluation of BC. However, the applicability of these receptors is still limited due to tumor heterogeneity [5]. Thus, it is necessary to identify new biomarkers for accurate evaluation of the prognosis of patients with cancers. Proper prediction of prognosis allows for selection of appropriate treatment plan and avoid the burden of overtreatment or undertreatment. In recent years, LncRNAs have been found to play an important role in BC tumor progression. LncRNAs are a class of RNA transcripts with more than 200 nucleotides [6]. Like proteins, mRNAs, and miRNAs, lncRNAs are considered to be novel independent biomarkers for early diagnosis and prediction of prognosis of patients with cancer. For instance, previous studies have shown that lncRNA HOTAIR can be used as a prognostic marker in breast cancer, Hepatocellular Carcinoma (HCC), gastric carcinoma, and Gastrointestinal Stromal Tumor (GIST), because it is highly expressed in the cancers and associated with poor prognosis [7-10].

RNA sequencing (RNA-Seq) technique is often used to analyze the biological behavior of different cells by observing their differences at the genetic level. Previously, results from RNA-seq were used to develop models for the diagnosis, treatment, and prognosis of BC. A study conducted by Ma et al. developed an immune-related lncRNA signature to improve the prognosis prediction of breast cancer based on the TCGA database [11]. According to Li et al. lncRNAs HIF1A - AS2, which is one of the three antisense genes of HIF-1α, up-regulates HIF-1α by sponging to miR-153-3p, thereby promoting angiogenesis in HUVECs under hypoxia conditions [12].

Wang et al. reported that the long noncoding RNA HIF1A-AS2 was upregulated in TNBC tissues and was associated with poor prognosis in triple-negative breast cancer [13]. Similarly, HIF1A-AS3 is also one of the three antisense genes of HIF-1A. A recent study revealed that HIF1A-AS3 can physically interact with Y-Box Binding Protein 1 (YBX1), suppressing the transcriptional expression of p21 and AJAP1 under hypoxic conditions, thereby promoting the development of ovarian cancer [14]. In another study, it was found that in breast cancer cells, induction of HIF1A-AS3 stabilizes the binding of HIF1A to the Hypoxia Response Element (HRE) by assembling the HIF1A transactivation complex, thereby enhancing the expression of HIF1α target genes [15]. Studies on the association of HIF1A-AS3 with human diseases have been carried out. We chose to study HIF1A-AS3 instead of HIF1A-AS1 because recent research indicates that, in a hypoxic environment, HIF1A-AS3 can promote ovarian cancer development through unique molecular mechanisms. Since hypoxia is also present in the progression of breast cancer and the role of HIF1A-AS3 in breast cancer has not been studied, we opted to investigate its involvement in this context. Through in-depth investigations of HIF1A-AS3, we aim to provide a comprehensive and profound understanding to contribute to the prognostic assessment and development of therapeutic strategies for breast cancer. However, the prognostic and therapeutic value of HIF1A-AS3 in BC is not well understood.

To the best of our knowledge, this study is the first to demonstrate the association of HIF1A-AS3 with poor prognosis of BC. Breast cancer cells and tissues from clinical patients were used to explore differences in HIF1A-AS3 expression between tumor tissues and normal samples as well as examine its prognosis value in BC using BC RNA-seq data in TCGA database. Further, we explored and discussed the potential mechanism by which HIF1A-AS3 modulates the occurrence and development of BC by investigating the correlation between HIF1A-AS3 expression and immune infiltration.

Materials and methods

Primary human breast cancer cell isolation and culture

Excised human breast cancer tissue obtaining during surgery was transferred to a biosafety cabinet. It was soaked in 75% ethanol for 1 min and then rinsed repeatedly with PBS containing P/S (penicillin/streptomycin) until the washing solution became clear. Fat, blood vessels, and other tissues were removed using ophthalmic scissors. The remaining tissue was cut into small pieces, washed, and digested overnight at 4°C using 0.1% type IV collagenase along with 0.1% dispase. The next day, the tissue and digestion solution were centrifuged, and the supernatant was discarded. The pellet was resuspended and further digested with 0.1% type IV collagenase at 37°C while agitating for 2-3 h. The mixture was filtered using a 100-mesh sieve. The filtrate was centrifuged at 300 g for 5 min, resuspended, and incubated in a 37°C, 5% CO_2 incubator.

Tissue samples

12 cases of human BC tissues and matched para-cancerous tissues used in this study were obtained from the Department of Breast Surgery, Shanghai Tongji Hospital (Shanghai, China) with the approval of the Ethics Committee of Shanghai Tongji Hospital. Written consent was obtained from the patients. BC tissues and matched para-cancerous tissues were cryopreserved in liquid nitrogen for temporary storage. The study was conducted in accordance with the Declaration of Helsinki (as revised in 2013), and approved by the ethics board of Shanghai Tongji Hospital, Shanghai, China (No. SBKT-2024-043). All study participants have written informed consent.

Cell culture

Human breast cancer cell lines MCF7, MDA-MB-231, BT549, and MDA-MB-468, and human normal breast epithelial cell line MCF10A were purchased from the Chinese Academy of Science, Shanghai (China). The MCF7, MDA-MB-231cells were cultured in DMEM medium with high glucose (Gibco, Thermo Fisher Scientific, Waltham, MA, USA), while the BT549 and MCF10A cells were cultured in RPMI-1640 medium (Gibco, USA) and mammary epithelial cell medium (Procell, Wuhan, China), respectively. The

growth media were enriched with 10% fetal bovine serum (Gibco, USA) and 100 U/mL penicillin and 100 μg/mL streptomycin (Servicebio, Wuhan, China). A 0.25% trypsin EDTA solution (Servicebio, China) was also applied for cell passaging. All cell lines were cultured in a cell incubator at 37°C and 5% CO_2.

RNA isolation, cDNA generation, and quantitative reverse transcription PCR

Total RNA of BT549, MCF-7, MDA-MB-231, MCF10A primary breast cancer and primary breast epithelial cells was isolated using the RNAiso Plus Kit (cat. no. 9109; Takara Biotechnology Co., Ltd.) according to the manufacturer's protocols. 1,000 ng mRNA was reverse transcribed into cDNA using the PrimeScriptTM RT Reagent Kit with the genomic DNA Eraser (cat. no. RR047; Takara Biotechnology Co., Ltd.) according to the manufacturer's protocols. Quantitative PCR (qPCR) analysis was performed in the LightCycler® 96 Instrument (Roche Diagnostics) using the TB Green Premix Ex Taq (cat. no. RR420; Takara Biotechnology Co., Ltd.) to detect the expression of each of the target genes. The following thermocycling conditions were used for qPCR: 95°C for 5 min, followed by 40 cycles of 95°C for 10 sec and 60°C for 30 sec. The qPCR primers, synthesized by Rui Mian Biological Technology (China), were as follows: HIF1A-AS3-F: GTCTTTCCTCTCCGTCCCAG and HIF1A-AS3-R: CAGACACCCGATCTCCGTG. For GAPDH, the primers used were GAPDH-F: CATTGACCTCAACTACATGGTTT and GAPDH-R: GAAGATGGTGATGGGATT-TCC. The housekeeping gene human glyceraldehyde 3-phosphate dehydrogenase (GAPDH) served as an endogenous control, and the relative mRNA expression levels were quantified using the 2-ΔΔCt method. All qRT-PCR experiments were conducted in triplicate.

RNA-sequencing data and bioinformatics analysis

Normalized RNA-seq data and corresponding clinical characteristics were collected from the TCGA-breast invasive carcinoma (TCGA-BRCA) datasets (https://tcga.xenahubs.net). Information from 1222 patients with BRCA were obtained. The format of the downloaded data was converted from level 3 HTSeq-Fragments Per Kilobase per Million (FPKM) into Transcripts Per Million (TPM) format for subsequent analysis. TCGA's database is open to the public under specific guidelines which confirms that all written informed consents were obtained prior to data collection. The XIAN-TAO platform (www.xiantao.love) was used to conduct a paired comparison between HIF1A-AS3 expression in BC and case-matched adjacent benign tissues obtained from the TCGA database.

Differentially expressed genes in BC

The 1222 BC patients were categorized into high and low HIF1A-AS3 expression groups according to HIF1A-AS3 median value. The R package "DESeq2" (v1.26.0) was used to identify Differentially Expressed Genes (DEGs) between the two groups through a two-tailed hypothetical test and based on the negative binomial generalized linear models, whereby the log-fold change larger than 1.5 and an adjusted *P*-value less than 0.05 were set as the thresholds. The obtained results were presented as heatmaps and volcano plots using R packages "pheatmap" [16] and "EnhancedVolcano"[17]. The heat maps of the DEGs were visualized using the "ggplot2" (v3.3.3) R package.

Tumor immune estimation resource database analysis

The immune infiltration analysis of BRCA was performed using single-sample GSEA (ssGSEA) with the GSVA package in R (3.6.2) (https://www.bioconductor.org/packages/release/bioc/html/GSVA. html) for 24 types of immune cells in the tumor samples. WilCoxon rank sum tests were used to reveal the association of the infiltration of immune cells with the groups with different levels of expression of HIF1A-AS3. Furthermore, the levels of immune cell infiltration were compared between the high and low HIF1A-AS3 expression groups using the Wilcoxon rank sum test.

Clinical significance of HIF1A-AS3 expression in BC

The Kaplan-Meier plotter Database (http://kmplot.com/analysis/) was used for survival analysis [18]. We used the pattern of mRNA of gene chip in breast cancer to explore the clinical prognostic value of HIF1A-AS3, including Overall Survival (OS), Disease-Specific Survival (DSS) and Progression-Free Interval (PFI) for patients with TCGA. The Hazard Ratio (HR) and 95% Confidence Interval (CI) were calculated and the differences between the survival curves were examined using log-rank tests. The R package "randomForest" [19] was used for random forest regression, whereas the R package "forestplot" [20] was employed to analyze the clinicopathological subgroup. All statistical analyses in the present study were performed using R version 3.6.3 (http://www.r-project.org/). P-value less than 0.05 was considered statistically significant.

Results

Expression of HIF1A-AS3 and related differentially expressed genes in BC

The expression level of HIF1A-AS3 in BC was analyzed on the 2021 TCGA database. A total of 1222 patients with BC were enrolled and stratified into two groups, high and low HIF1A-AS3 expression groups. It was found that, although the expression level of HIF1A-AS3 was higher in BC tissue as compared with the normal tissue, difference was not statistically significant between the two groups (Supplementary Figure 1).

Further, the expression of mRNA and lncRNA was compared between the two groups. Results showed that 183 mRNAs including 165 upregulated and 18 downregulated mRNAs as well as 793 lncRNAs which included 785 upregulated and 8 downregulated lncRNAs were recognized as DEGs (absolute value of fold change>1.5, P<0.05) in the high HIF1A-AS3 group. Moreover, representative DEGs were displayed on heatmaps (Figures 1A-D). Surprisingly, RT-qPCR analysis revealed that HIF1A-AS3 was highly expressed in breast cancer cells especially MCF7, MDA-MB 468 cell but not in MDA-MB-231 and BT549, compared with normal breast cell (MCF10A) (Figure 1E). In addition, higher expression level of HIF1A-AS3 was found in 12 breast cancers tissues compared to matched paracancerous tissues from clinical patient samples (Figure 1F). The expression level of HIF1A-AS3 was higher in primary breast cancer cell than primary breast epithelial cell (normal) (Figure 1G). These results suggested that HIF1A-AS3 may be an important lncRNA driving the development of BC.

Predictive value of HIF1A-AS3 for BC

KM analyses were performed to verify the prediction value of HIF1A-AS3 for clinical outcomes. The study unveiled notable

discrepancies in OS (HR: 1.42 (1.04-1.96), P=0.029) (Figure 2A), PFI (HR: 1.60 (1.15-2.23), P=0.005) (Figure 2B), and DSS (HR: 1.60 (1.04-2.45), P=0.031) (Figure 2C) between the high and low HIF1A-AS3 expression groups. In addition, we extended our investigation to various other cancer types. The results established a significant link between HIF1A-AS3 expression and diminished OS of patients diagnosed with lung adenocarcinoma, thyroid carcinoma, stomach adenocarcinoma, colon adenocarcinoma, and glioblastoma multiforme (Supplementary Figure 2).

Prognostic performance of HIF1A-AS3 in BC clinicopathological subgroups

In addition, we evaluated the predictive value of HIF1A-AS3 for clinical outcomes in several clinicopathological subgroups. Cox regression analyses was carried out in specific subgroups and results were presented as forest plots. The forest plot showed that HIF1A-AS3 was a significant risk factor for OS in patients with pathological stages III and IV (HR=2.21, P=0.037), age below 60 years (HR=1.84, P=0.039), clinical T1 and T2 stage (HR=1.71, P=0.0035), clinical N, 1N2 and N3 stages (HR =1.64, P=0.05) and clinical M0 stage (HR=1.65, P=0.046) (Figure 3A). Similar observations were noted for PFI in patients with pathological stage III and IV (HR=1.88, P=0.021), age below 60 years (HR=1.88, P=0.009), clinical T1&T2 stage (HR=1.47, P=0.046), clinical N1, N2 and N3 stages (HR =1.5, P=0.049) and clinical M0 stage (HR=1.41, P=0.059) (Figure 3B). Further, the HIF1A-AS3 was found to be a significant risk factor for DSS in patients with pathological stage III&IV (HR=1.74, P=0.059), below the age of 60 years (HR=1.81, P=0.008), clinical T1 and T2 stage (HR=1.56, P=0.024), clinical N1&N2&N3 stages (HR =1.48, P=0.058) and clinical M0 stage (HR=1.77, P=0.003) (Figure 3C).

The KM analyses of clinical outcomes (OS, PFS, and DSS) were also presented in three representative subgroups: clinical stages T1and T2, aged below 60, as well as the pathological stages III and IV (Figure 4). It was evident that the findings of all analyses in the present study indicated a significant improvement in clinical outcomes for patients with low expression of HIF1A-AS3.

Correlation between HIF1A-AS3 expression and immune infiltration

In this study, we initially employed ssGSEA to investigate the association of HIF1A-AS3 expression with immune infiltration. Our analysis identified 24 distinct immune cell types in breast cancer. Subsequently, we examined the correlation between HIF1A-AS3 and the infiltration of immune cells using Spearman's correlation. A positive association was found between expression of HIF1A-AS3 and Tcm (R=0.276, P<0.001), Th1 cells (R=0.190, P<0.001), Th2 cells (R=0.161, P<0.001), aDC (R=0.0115, P<0.001), Macrophage (R=0.0269, P<0.001), and Neutrophils (R=0.143, P<0.001). On the other hand, NK cells (R=-0.231, P<0.001), CD8 T cells (R=-0.166, P<0.001), and pDC cells (R=-0.161, P<0.001) were negatively association with expression level of HIF1A-AS3.
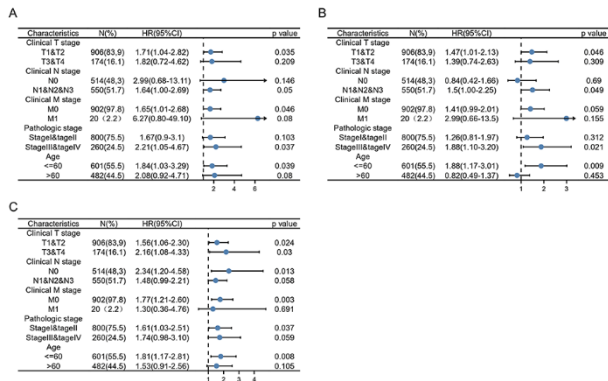
The levels of infiltration of six important immune cells-Tcm, neutrophils (Figure 5C), macrophages (Figure 5D), Nk cells (Figure 5E), CD8 T cells (Figure 5F), pDC (Figure 5G), Th2 cells (Figure 5H), and Th cells (Figure 5I) in distinct HIF1A-AS3 groups were analyzed. It was observed that the results were in agreement with those shown in Figure 5A.
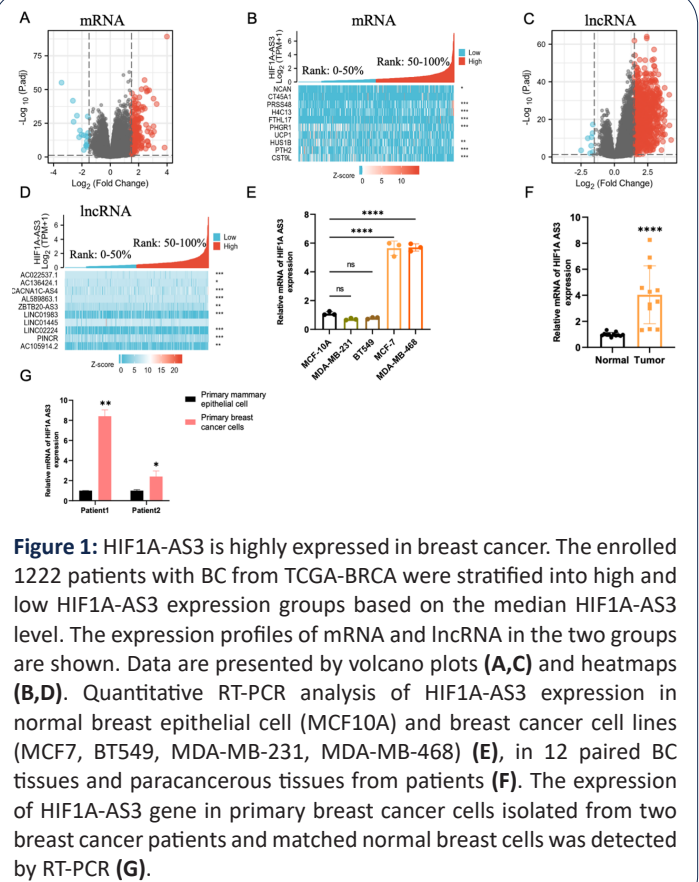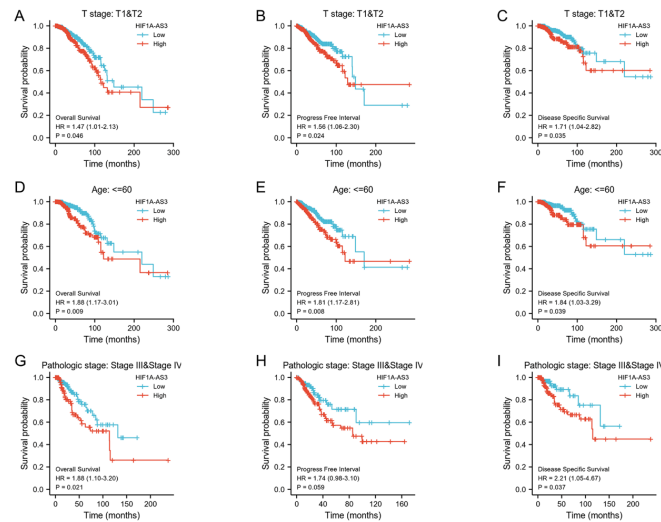

Figure 1: HIF1A-AS3 is highly expressed in breast cancer. The enrolled 1222 patients with BC from TCGA-BRCA were stratified into high and low HIF1A-AS3 expression groups based on the median HIF1A-AS3 level. The expression profiles of mRNA and lncRNA in the two groups are shown. Data are presented by volcano plots **(A,C)** and heatmaps **(B,D)**. Quantitative RT-PCR analysis of HIF1A-AS3 expression in normal breast epithelial cell (MCF10A) and breast cancer cell lines (MCF7, BT549, MDA-MB-231, MDA-MB-468) **(E)**, in 12 paired BC tissues and paracancerous tissues from patients **(F)**. The expression of HIF1A-AS3 gene in primary breast cancer cells isolated from two breast cancer patients and matched normal breast cells was detected by RT-PCR **(G)**.
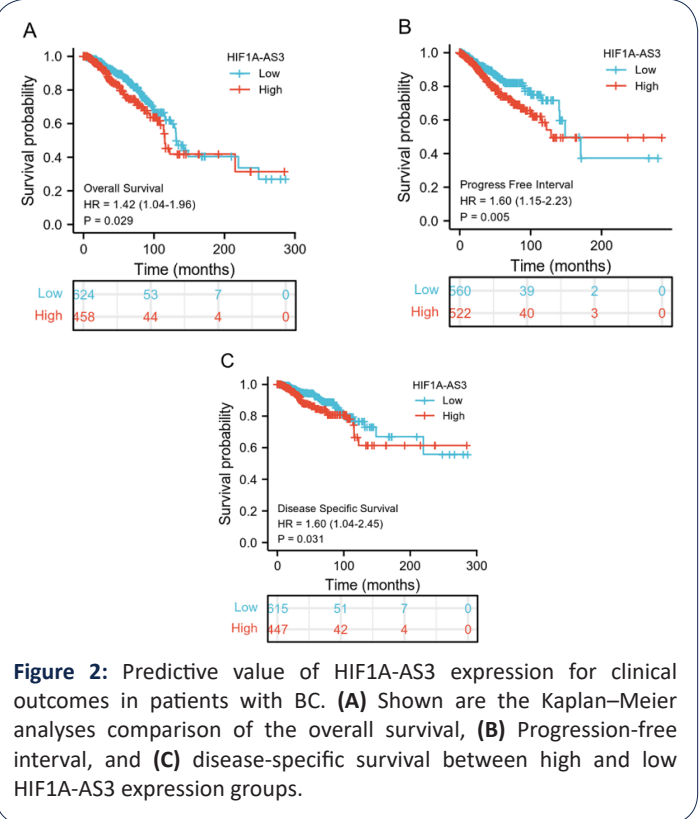
Figure 2: Predictive value of HIF1A-AS3 expression for clinical outcomes in patients with BC. **(A)** Shown are the Kaplan–Meier analyses comparison of the overall survival, **(B)** Progression-free interval, and **(C)** disease-specific survival between high and low HIF1A-AS3 expression groups.

Figure 3 (A)

Characteristics	N(%)	HR(95%CI)	p value
Clinical T stage			
T1&T2	906(83.9)	1.71(1.04-2.82)	0.035
T3&T4	174(16.1)	1.82(0.72-4.62)	0.209
Clinical N stage			
N0	514(48.3)	2.99(0.68-13.11)	0.146
N1&N2&N3	550(51.7)	1.64(1.00-2.69)	0.05
Clinical M stage			
M0	902(97.8)	1.65(1.01-2.68)	0.046
M1	20 (2.2)	6.27(0.80-49.10)	0.08
Pathologic stage			
StageI&stageII	800(75.5)	1.67(0.9-3.1)	0.103
StageIII&stageIV	260(24.5)	2.21(1.05-4.67)	0.037
Age			
<=60	601(55.5)	1.84(1.03-3.29)	0.039
>60	482(44.5)	2.08(0.92-4.71)	0.08

Figure 3 (B)

Characteristics	N(%)	HR(95%CI)	p value
Clinical T stage			
T1&T2	906(83.9)	1.47(1.01-2.13)	0.046
T3&T4	174(16.1)	1.39(0.74-2.63)	0.309
Clinical N stage			
N0	514(48.3)	0.84(0.42-1.66)	0.69
N1&N2&N3	550(51.7)	1.5(1.00-2.25)	0.049
Clinical M stage			
M0	902(97.8)	1.41(0.99-2.01)	0.059
M1	20 (2.2)	2.99(0.66-13.5)	0.155
Pathologic stage			
StageI&stageII	800(75.5)	1.26(0.81-1.97)	0.312
StageIII&stageIV	260(24.5)	1.88(1.10-3.20)	0.021
Age			
<=60	601(55.5)	1.88(1.17-3.01)	0.009
>60	482(44.5)	0.82(0.49-1.37)	0.453

Figure 3 (C)

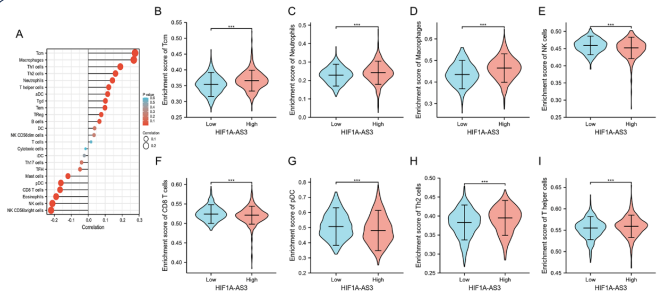| Characteristics	N(%)	HR(95%CI)	p value
Clinical T stage			
T1&T2	906(83.9)	1.56(1.06-2.30)	0.024
T3&T4	174(16.1)	2.16(1.08-4.33)	0.03
Clinical N stage			
N0	514(48.3)	2.34(1.20-4.58)	0.013
N1&N2&N3	550(51.7)	1.48(0.99-2.21)	0.058
Clinical M stage			
M0	902(97.8)	1.77(1.21-2.60)	0.003
M1	20 (2.2)	1.30(0.36-4.76)	0.691
Pathologic stage			
StageI&stageII	800(75.5)	1.61(1.03-2.51)	0.037
StageIII&stageIV	260(24.5)	1.74(0.98-3.10)	0.059
Age			
<=60	601(55.5)	1.81(1.17-2.81)	0.008
>60	482(44.5)	1.53(0.91-2.56)	0.105

Figure 3: Prognostic performance of HIF1A-AS3 on clinical outcomes in different subgroups of patients with BC. Patients were divided into different subgroups based on age, clinical TNM stage, and clinical pathologic stage. For each subgroup, the prognostic performance of HIF1A-AS3 on overall survival **(A)**, progression-free interval **(B)**, and disease-specific survival **(C)** were evaluated using Cox regression, and the results are presented as hazard ratio. The bar represents 95 % confidence interval of hazard ratio, the diamond's size represents the significance of HIF1A-AS3's performance.

Figure 5: Correlation of immune cell infiltration and HIF1A-AS3 expression in patients with BC. **(A)** Relationships among infiltration levels of 24 immune cell types and HIF1A-AS3 expression profiles by Spearman's analysis. Comparison of infiltration levels of the most correlated immune cells, including Tcm **(B)**, neutrophils **(C)**, macrophages **(D)**, NK cells **(E)**, CD8 T cells **(F)**, plasmacytoid DCs (pDC) **(G)**, type 2 T helper cells (Th2) cells **(H)**, and Th cells **(I)** between high and low HIF1A-AS3 expression groups is shown. DCs, dendritic cells; aDCs, activated DCs; iDCs, immature DCs; pDCs, plasmacytoid DCs; Th, T helper cells; Th1, type 1 Th cells; Th2, type 2 Th cells; Th17, type 17 Th cells; Treg, regulatory T cells; Tgd, T gamma delta; Tcm, T central memory; Tem, T effector memory; Tfh, T follicular helper; NK, natural kill. ns, $P \geq 0.05$; *$P<0.05$; **$P<0.01$; ***$P<0.001$.
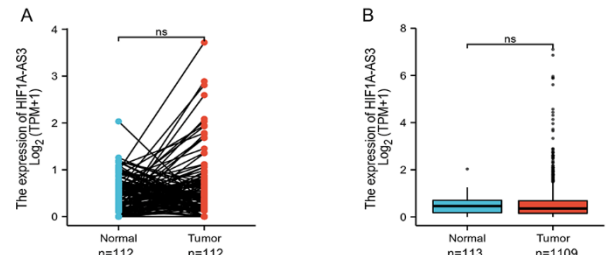
Figure 4: Distinct clinical outcomes associated with HIF1A-AS3 expression in subgroups of patient with BC. Kaplan-Meier analysis showing the comparison of overall survival **(A,D,G)**, progression-free interval **(B,E,H)**, and disease-specific survival **(C,F,I)** between high and low HIF1A-AS3 expression groups in several BC patient subgroups, including T stages T1–T2 **(A-C)**, age below 60 years **(D–F)**, and pathologic stage III-IV **(G-I)**.

Supplementary Figure 1: (A) Wilcoxon rank sum test was used to analyze differences in HIF1A-AS3 expression between BC tissues and adjacent breast tissues from TCGA database. **(B)** Wilcoxon signed rank sum test was used to quantify differences in expression of HIF1A-AS3 between BC tissues and adjacent breast tissues from TCGA database. ns, $P \geq 0.05$; *$P<0.05$; **$P<0.01$; ***$P<0.001$.
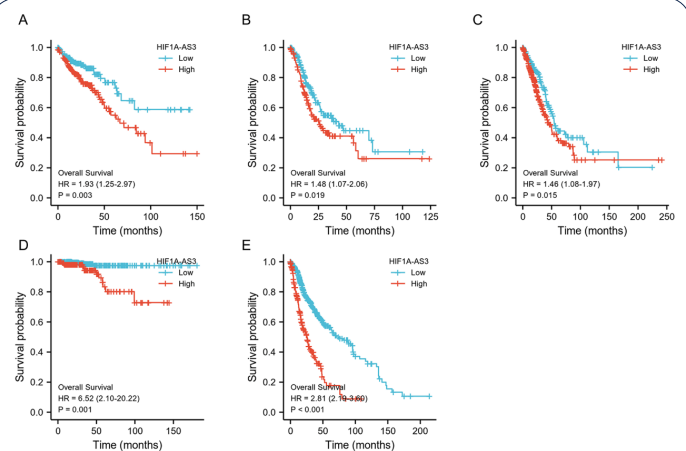
Discussion

The present study analyzed the datasets from the TCGA-BRCA project to investigate the expression profiles and prognostic value of HIF1A-AS3 in BC. The differential expression of HIF1A-AS3 in breast cancer was explored at the cellular level and clinical tissue samples. We found that HIF1A-AS3 exhibited good predictive value for OS, PFI, and DSS in patients with BC, especially in those of age below 60 years, clinical T stages T1-T2 and pathologic stages III -IV.

Supplementary Figure 2: Expression and prognosis value of HIF1A-AS3 in patients with other cancers. Kaplan-Meier curve was drawn using the R package survminer to evaluate the association of HIF1A-AS3 with OS of some other cancer types. HIF1A-AS3 expression value was divided into high and low expression group according to median value. **(A)** Colon adenocarcinoma, **(B)** Stomach adenocarcinoma, **(C)** Lung adenocarcinoma, **(D)** Thyroid carcinoma, and **(E)** Glioblastoma multiforme.

Long noncoding RNAs (lncRNAs) are transcripts with more than 200 nucleotides long, with no open reading frame. The role of lncRNA in tumor progression has attracted increasing attention in recent years [21]. To the best of our knowledge, HIF1A-AS3 is one of three antisense genes for HIF1A [22]. However, only HIF1A-AS1 and HIF1A-AS2 have been extensively studied.

Previous studies have shown that HIF1A-AS2 is aberrantly expressed in various human cancers (such as epithelial ovarian cancer, colorectal cancer, osteosarcoma, breast cancer, and glioblastoma) and is involved in the progression and metastasis of the tumors [23-28]. A recent study reported that the HIF1A-AS1 gene upregulated HIF1A expression, promoted glycolysis, and enhanced GEM resistance in pancreatic cancer cells [29].

The mechanism driving this phenomenon involves the interaction between serine/threonine kinase AKT and Y-Box-Binding protein 1 (YB1), which in turn promotes phosphorylation of YB1 (pYB1). HIF1A-AS1 recruits pYB1 to HIF1a mRNA thereby promoting the translation of HIF1a. Furthermore, HIF1a promotes transcription of HIF1A-AS1 by directly binding to the response element of HIF1a in the promoter area of HIF1A-AS1 and hence form positive feedback [22].

However, little is known about the relationship between HIF1A-AS3 and cancer. In this study, the differences in expression levels of HIF1A-AS3 between BC and normal tissues were not significant. Results showed that high expression of HIF1A-AS3 was significantly associated with poor outcomes. Moreover, we found that HIF1A-AS3 may have a similar function as HIF1A-AS2.

The Kaplan-Meier analyses demonstrated that patients with high expression of HIF1A-AS3 was associated with shorter OS, DSS, and PFI compared to those with low HIF1A-AS3 expression. This suggests that HIF1A-AS3 could serve as a valuable prognostic biomarker for breast cancer patients. Additionally, elevated levels of HIF1A-AS3 were associated with specific clinicopathological characteristics, including younger age, clinical T stages T1-T2, and pathological stages III-IV. These findings indicate that high HIF1A-AS3 expression not only predicts prognosis in early-stage breast cancer but also serves as a prognostic indicator for advanced stages. In addition, this study also showed a latent correlation between HIF1A-AS3 expression and immune cell infiltration. It was evident that expression of HIF1A-AS3 is negatively correlated with pDC, CD8+T cells, NK cells, and eosinophils. Plasmacytoid Dendritic Cells (pDC) are specialized producers of type I interferon (IFN-I) that promote antiviral and antitumor immunity [30]. CD8+T cells are key mediators of the function of cytotoxic effector in infection, cancer. Furthermore, autoimmunity and exhaustion of CD8+T cells in tumor microenvironment is often considered to be one of the factors leading to poor immunotherapy efficacy [31,32].

Moreover, NK cells play an immunological surveillance role in tumors and may attract the infiltration of T cell through secretion of cytokines and chemokines to induce antitumor responses [33]. Therefore, high expression of HIF1A-AS3 may impair the antitumor immune response leading to tumor progression. Meanwhile, our results showed that high expression of HIF1A-AS3 is accompanied by increased infiltration of Tcm. Tumor-infiltrating Tcm cells often display a dysfunctional phenotype associated with tumor progression and this may explain the transition from antitumor

response to non-response of Tcm cells because of excessive exposure to neoantigen [34,35]. Moreover, it has been previously found that Tcm cells are associated with the recurrence of prostate cancer after radical resection [36]. To the best of our knowledge, this study is the first to provide multilevel evidence for the significance of HIF1A-AS3 in the BC and its potential as a prognostic biomarker for BC.

This study found that high HIF1A-AS3 expression in breast cancer is associated with poor overall survival, progression-free interval, and disease-specific survival, especially in younger patients and those with early clinical or advanced pathological stages. Additionally, HIF1A-AS3 negatively correlates with immune cell infiltration, suggesting a role in tumor progression.

This study had some limitations. First, there are few studies on HIF1A-AS3 and the specific pathway of HIF1A-AS3 in occurrence and progression of cancer is still unclear. Second, we exclusively validated the expression levels of HIF1A-AS3 in breast cancer through *in vitro* experiments, and the data in this paper were mainly derived from the results of bioinformatics analysis. Therefore, further verification is needed through *in vivo* experiments. Finally, the TCGA database is updated frequently, the results are sometimes wobble, and it is common for different genes to be expressed differently in different diseases. In the future, large clinical sample data are needed to further validate our results. In conclusion, explorative studies focusing on the definitive function and mechanism via which HIF1A-AS3 affects prognosis of BC patients are advocated.

Declarations

References

1. Siegel RL, et al. Cancer Statistics. CA Cancer J Clin. 2021; 71(1): 7-33.

2. Siegel RL, et al. Cancer statistics. CA Cancer J Clin. 2022; 72(1): 7-33.

3. Nandi A, R Chakrabarti. The many facets of Notch signaling in breast cancer: Toward overcoming therapeutic resistance. Genes Dev. 2020; 34(21-22): 1422-1438.

4. Munoz D, et al. Effects of screening and systemic adjuvant therapy on ER-specific US breast cancer mortality. J Natl Cancer Inst. 2014; 106(11): 2-3.

5. Barzaman K, et al. Breast cancer: Biology, biomarkers, and treatments. Int Immunopharmacol. 2020; 84: 106535.

6. Kopp F, JT Mendell. Functional Classification and Experimental Dissection of Long Noncoding RNAs. Cell. 2018; 172(3): 393-407.

7. Gupta RA, et al. Long non-coding RNA HOTAIR reprograms chromatin state to promote cancer metastasis. Nature. 2010; 464(7291): 1071-6.

8. Kogo R, et al. Long noncoding RNA HOTAIR regulates polycomb-dependent chromatin modification and is associated with poor prognosis in colorectal cancers. Cancer Res. 2011; 71(20): 6320-6.

9. Zhang J, et al. HOTAIR contributes to the carcinogenesis of gastric cancer via modulating cellular and exosomal miRNAs level. Cell Death Dis. 2020; 11(9): 780.

10. Zhang J, et al. LncRNA-HOTAIR activates autophagy and promotes the imatinib resistance of gastrointestinal stromal tumor cells through a mechanism involving the miR-130a/ATG2B pathway. Cell Death Dis. 2021; 12(4): 367.

11. Ma W, et al. Immune-related lncRNAs as predictors of survival in breast cancer: A prognostic signature. J Transl Med. 2020; 18(1): 442.

12. Li L, et al. lncRNAs HIF1A-AS2 facilitates the up-regulation of HIF-1α by sponging to miR-153-3p, whereby promoting angiogenesis in HUVECs in hypoxia. Biomed Pharmacother. 2017; 96: 165-172.

13. Wang Y, G Zhang, J Han. HIF1A-AS2 predicts poor prognosis and regulates cell migration and invasion in triple-negative breast cancer. J Cell Biochem. 2019; 120(6): 10513-10518.

14. Xie W, et al. A novel hypoxia-stimulated lncRNA HIF1A-AS3 binds with YBX1 to promote ovarian cancer tumorigenesis by suppressing p21 and AJAP1 transcription. Mol Carcinog. 2023; 62(12): 1860-1876.

15. Zheng F, et al. The HIF-1α antisense long non-coding RNA drives a positive feedback loop of HIF-1α mediated transactivation and glycolysis. Nat Commun. 2021; 12(1): 1341.

16. Xia S, et al. Increased Expression of TICRR Predicts Poor Clinical Outcomes: A Potential Therapeutic Target for Papillary Renal Cell Carcinoma. Front Genet. 2020; 11: 605378.

17. Blighe K. Publication-ready volcano plots with enhanced colouring and labeling. 2022; 5: 2-7.

18. Lánczky A, et al. Mir power: A web-tool to validate survival-associated miRNAs utilizing expression data from 2178 breast cancer patients. Breast Cancer Res Treat. 2016; 160(3): 439-446.

19. Svetnik V, et al. Random forest: A classification and regression tool for compound classification and QSAR modeling. J Chem Inf Comput Sci. 2003; 43(6): 1947-58.

20. Fang Y, et al. Comprehensive Analysis of Peritoneal Metastasis Sequencing Data to Identify LINC00924 as a Prognostic Biomarker in Gastric Cancer. Cancer Manag Res. 2021; 13: 5599-5611.

21. Liu Y, et al. lncRNA HIF1A-AS2: A potential oncogene in human cancers (Review). Biomed Rep. 2021; 15(4): 85.

22. Rodriguez-Lorenzo S, et al. Altered secretory and neuroprotective function of the choroid plexus in progressive multiple sclerosis. Acta Neuropathol Commun. 2020; 8(1): 35.

23. Chen WM, et al. Antisense Long Noncoding RNA HIF1A-AS2 Is Upregulated in Gastric Cancer and Associated with Poor Prognosis. Dig Dis Sci. 2015; 60(6): 1655-62.

24. Lin H, et al. Long noncoding RNA HIF1A-AS2 facilitates cell survival and migration by sponging miR-33b-5p to modulate SIRT6 expression in osteosarcoma. Biochem Cell Biol. 2020; 98(2): 284-292.

25. Wu D, et al. lncRNA HIF1A Antisense RNA 2 Modulates Trophoblast Cell Invasion and Proliferation through Upregulating PHLDA1 Expression. Mol Ther Nucleic Acids. 2019; 16: 605-615.

26. Lin J, et al. LncRNA HIF1A-AS2 positively affects the progression and EMT formation of colorectal cancer through regulating miR-129-5p and DNMT3A. Biomed Pharmacother. 2018; 98: 433-439.

27. The Inhibitive Effect of sh-HIF1A-AS2 on the Proliferation, Invasion, and Pathological Damage of Breast Cancer via Targeting miR-548c-3p Through Regulating HIF-1α/VEGF Pathway in vitro and vivo [Retraction]. Onco Targets Ther. 2021; 14: 1003.

28. Zhang W, et al. Long Noncoding RNA HIF1A-AS2 Promotes Non-Small Cell Lung Cancer Progression by the miR-153-5p/S100A14 Axis. Onco Targets Ther. 2020; 13: 8715-8722.

29. Xu F, et al. LncRNA HIF1A-AS1 Promotes Gemcitabine Resistance of Pancreatic Cancer by Enhancing Glycolysis through Modulating the AKT/YB1/HIF1α Pathway. Cancer Res. 2021; 81(22): 5678-5691.

30. Greene TT, YR Jo, EI Zuniga. Infection and cancer suppress pDC derived IFN-I. Curr Opin Immunol. 2020; 66: 114-122.

31. Collier JL, et al. Not-so-opposite ends of the spectrum: CD8(+) T cell dysfunction across chronic infection, cancer and autoimmunity. Nat Immunol. 2021; 22(7): 809-819.

32. Hossain MA, et al. Reinvigorating exhausted CD8(+) cytotoxic T lymphocytes in the tumor microenvironment and current strategies in cancer immunotherapy. Med Res Rev. 2021; 41(1): 156-201.

33. Shimasaki N, A Jain, D Campana. NK cells for cancer immunotherapy. Nat Rev Drug Discov. 2020; 19(3): 200-218.

34. Reading JL, et al. The function and dysfunction of memory CD8(+) T cells in tumor immunity. Immunol Rev. 2018; 283(1): 194-212.

35. Merad M, et al. The dendritic cell lineage: ontogeny and function of dendritic cells and their subsets in the steady state and the inflamed setting. Annu Rev Immunol. 2013; 31: 563-604.

36. Rui X, et al. Identification of recurrence marker associated with immune infiltration in prostate cancer with radical resection and build prognostic nomogram. BMC Cancer. 2019; 19(1): 1179.